

Effects of Sodium Octaborate on AISI 4140 Steel Machined by Die-sinking EDM

Daniel de Moraes Lima^a, Sinval Pedroso da Silva^{b*} , Claudinei Alfredo do Nascimento^a,

Ernane Rodrigues da Silva^a

^aCentro Federal de Educação Tecnológica de Minas Gerais, Programa de Pós-Graduação em Engenharia de Materiais (POSMAT), Av. Amazonas, 5253, Nova Suíça, 30480-000, Belo Horizonte, MG, Brasil.

^bInstituto Federal de Educação, Ciência e Tecnologia de Minas Gerais (IFMG), Departamento de Mecânica, Av. Michel Pereira de Souza, 3007, Campinho, 36415-000, Congonhas, MG, Brasil.

Received: July 09, 2022; Revised: September 08, 2022; Accepted: September 11, 2022

Researchers are constantly developing processes aiming to improve the properties of metal surfaces, especially related to the wear resistance of components, as in the case of the nitrided layer obtained by die-sinking electrical discharge machining (EDM). Following this line of research, this work investigated the effects of sodium octaborate ($\text{Na}_2\text{B}_8\text{O}_{13}\cdot 4\text{H}_2\text{O}$), mixed into deionized water as a dielectric fluid on AISI 4140 steel surfaces machined by die-sinking EDM. An adapted EDM machine was employed in the process using electrolytic copper as tool. The effects on AISI 4140 steel-machined surfaces were evaluated by optical microscopy, Vickers microhardness, X-ray diffraction, and energy dispersion X-ray spectroscopy (EDS) analyses. The results showed a hardness gain of approximately 146.8% in the modified layer when compared to the AISI 4140 steel (base material). This suggests the formation of a borided layer, such as the Fe_2B phases identified on sample surfaces, which can be explained by the boron element decomposed from the dielectric solution.

Keywords: AISI 4140 steel, Boriding, Dielectric solution; Die-sinking EDM, Sodium octaborate.

1. Introduction

For metals applications where better properties such as wear resistance and corrosion resistance are required, thermochemical treatments (e.g., carburizing, nitriding, and boriding) are generally applied¹. The boriding aims to diffuse boron (B) on the surface of metallic substrates. Due to its relatively small atomic radius of 87 picometers², the light boron atom diffuses into various metallic materials³. The diffusion of boron on the surface of metallic alloys creates a dense region of metallic borides, which effectively generates superior surface properties⁴. The borided layer combines high hardness with a low friction coefficient, which helps to combat the main wear mechanisms (e.g., adhesive, abrasive, and surface fatigue).

Several thermochemical boriding techniques are used on the surfaces of the metallic material such as diffusion by solid, liquid, and gaseous media⁵. In addition, physical techniques are also used, for example, boron ion implantation, glow discharge conditions, and high-energy techniques. According to Kulka⁵, in the boriding high-energy techniques, the high-energy electric field between the voltage supply source and the workpiece generates a beam that accelerates the ions, which deploy the boron as soon they collide with the surface. This thermochemical process provides the necessary conditions to create a boron-modified superficial layer with superior properties, especially related to the wear resistance of the component.

According to Sinha⁶, plasma boriding is applied in industry to increase the surface hardness of ferrous alloys. Plasma can be generated by passing an electrical current through a gas. Even a relatively small percentage of charge is enough to make it electrically conductive⁷. Plasma is an ionized gas, generally electrically neutral, consisting of molecules, atoms, ions, electrons, and photons⁸. Electrical charges are normally used to produce plasma through ionization⁹ in the same gas. The plasma treatments are associated with positive ions produced in the gas phase through electron-molecule collisions to the surface to be treated, which occurs through the bombardment of ions, electrons, and photons, produced in the plasma¹⁰. Figure 1 schematically illustrates the physical-chemical interactions that occurs between the substrate surfaces and the ions-plasma-metal interface¹¹.

The collisions of the accelerated electrons in the magnetic field provide enough energy to cause new collisions, and consequently maintain the electrical discharge and ionization of the plasma channel¹². The kinetic energy that the ions acquire is enough to promote the transport of chemical elements such as nitrogen and carbon that interacts physically and chemically with the surface undergoing diffusion treatment¹³. Plasma boriding enables the boron element diffusion on the surface of metals and metal alloys. The compounds formed on the surface are similar to those obtained by other boriding methods¹⁴. The interaction between the surface and the dissociation of the ionized gas from the plasma channel results in the release of positive ions that have sufficient

*e-mail: sinvalpedroso@yahoo.com.br

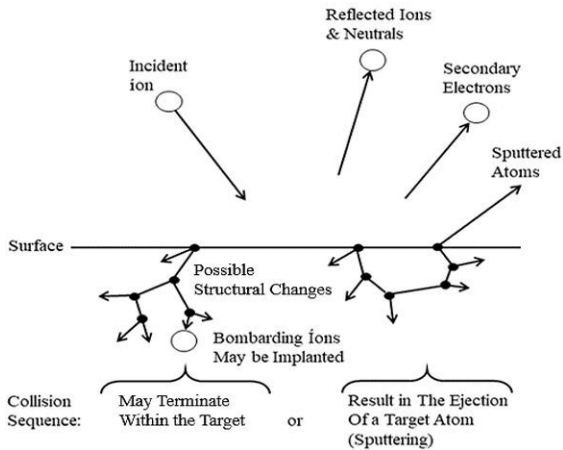


Figure 1. Schematic of ions with surfaces interaction [Adapted from Chapman and Vossen¹¹].

attractive force to move towards the treated surface¹⁵. The diffusion mechanism depends on the microstructural type of solution formed with the base metal and the relation between the size of the additional atoms and the size of the matrix's atoms¹⁶. Due to the small atomic size of the boron element, its diffusion in ferrous materials is favored¹⁷. Based on that, the atoms are transferred using thermal energy to the lattice of the parent material forming borides together with the atoms in the crystal lattice¹⁸. The flow of electrons and ions propagates rapidly between the electrodes along a path charged by a primary avalanche, which promotes the formation of more electrons and ions¹⁹.

Surface treatment of materials has been a subject of high interest in the scientific community. Several efforts have been employed in the findings of new techniques and/or different methods that can promote better and specific properties to surfaces¹⁷. Plasma electrolysis treatment is one of these methods, which consists of applying a voltage between two electrodes immersed in an electrolyte solution²⁰. Taktak²¹ used borax and boric acid to form an electrolyte solution and thus study the boriding process in AISI H13 tool steel. The plasma channel is created when an electric field is formed in the space between the electrodes. Once the plasma channel is stable, it concentrates the positive ions near the cathode, enabling electrical, thermal, and chemical interactions with the surface, and then, provides the conditions for the metallic surfaces treatments²². Figure 2 illustrates the schematic configuration of the deposition process of boron by plasma electrolysis on AISI 2365 steel used by²³.

According to Sireli²⁴, the process of boriding by electrolytic plasma is a promising alternative. The implantation of boron on the substrate occurs due to electrochemical reactions promoted by the electric current. During electrolytic plasma boriding, the diffusion and reaction of boron atoms with the metallic substrate form interstitial boron compounds, with a resulting layer consisting of metallic borides²⁵.

Electrical Discharge Machining (EDM) is a nonconventional machining process of electrically conductive material, which generates thermal energy through a plasma channel from each electrical discharge. During the EDM process, a portion of the material evaporates, and the other forms a

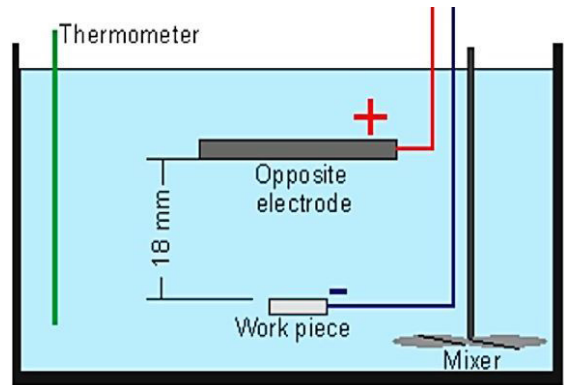


Figure 2. Schematic diagram of pulsed plasma electrolysis setup [Adapted from Akyüz and Tek²³].

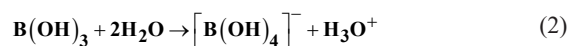
recast layer due to the cooling promoted by the dielectric fluid²⁶. Several theories have been formulated about the process of material removal by the EDM process. Among them, the thermoelectric theory is the most accepted by researchers, and according to König²⁷, that theory can be described as a sequence of four distinct steps: (a) ignition; (b) discharge; (c) plasma channel formation; (d) ejection and/or waste sublimation, as shown in Figure 3.

The steps takes place in the working gap between the two conducting electrodes submerged in the dielectric fluid. In the ignition phase (Figure 3a), the electrons released by the cathode accelerate and collide with the molecules that constitute the dielectric fluid. The collisions release other electrons and create ions, establishing a cycle of ionization by impact (Figure 3b). Then, the formation of the plasma channel occurs (Figure 3c) due to the energy released by the collision of electrons. The plasma channel is maintained during the discharge time, which is one of the adjustable parameters on the EDM machine. During the fusion phase, the cathode surface material starts to fuse due to the energy of intense bombardment by electrons and ions. At the end of the discharge time, the electric current is interrupted, and the plasma channel is abruptly broken, triggering the next phase, ejection (Figure 3d). The plasma channel causes the fusion and sublimation of the material surface, heated by the high energy of the plasma. However, the dielectric fluid does not completely remove the molten material, and part of it solidifies again in the cavity of the cathode, forming the recast layer²⁷.

Disodium octaborate tetrahydrate is an odorless white solid that converts to boric acid when dissolved in water, according to Equation 1:



In aqueous solutions of sodium octaborate tetrahydrate, chemical equilibrium is established where boric acid binds to the hydroxyl groups resulting from the auto-ionization of water molecules. At low boron concentrations ($\text{B} \leq 0.025 \text{ M}$), the equilibrium can be described according to Equation 2:



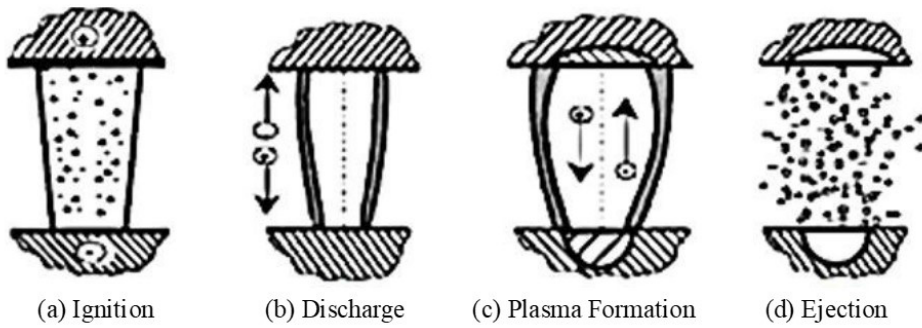
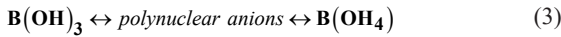
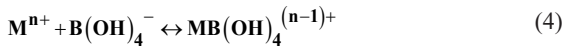


Figure 3. The phases of an electrical discharge in EDM [Adapted from König²⁷].

At higher boron concentrations ($B > 0.025$ M), the equilibrium is established between boric acid and more complex polynuclear anions, such as $B_3O_3(OH)_4^-$, $B_4O_5(OH)_4^{2-}$, $B_5O_6(OH)_4^{3-}$, $B_5O_6(OH)_5^{2-}$, $B_5O_6(OH)_4^{3-}$ and $B(OH)_4^-$. In summary, one can represent such conditions in Equation 3:



In the presence of metallic ions, such as Na^+ , Mg^{2+} , Ca^{2+} , etc., the equilibrium is shifted towards the formation of cation [metallic] + anion [borates], according to Equation 4:



The dielectric fluid is constituted by the aqueous solution of sodium octaborate tetrahydrate. The presence of Na^+ cations shifts the equilibrium in favor of dissociation, which decreases the concentration of molecular boric acid and increases the concentration of ions boron dissolved in the aqueous medium.

Regarding surface treatments, several researchers have studied surface modification through die-sinking electrical discharge machining (EDM), with significant improvements reported²⁸⁻³⁰. For instance²⁹, reported that the layer produced on the component surface machined by EDM was enriched with carbon from the hydrocarbon-based dielectric fluid due to the decomposition reaction. Researchers are interested in developing easily manageable and cost-effective surface modification technology^{30,31}. Thus, the main goal of this work was to evaluate the effects of sodium octaborate ($Na_2B_8O_{13} \cdot 4H_2O$) mixed into deionized water as dielectric fluid during the AISI 4140 steel machining by die-sinking EDM, employing electrolytic copper as a tool. It was used X-ray diffraction (XRD) to identify the formation of a borided layer, whose peaks from diffractograms were analyzed and compared to existing patterns⁵.

2. Experimental Procedure

This work was conducted on a conventional die-sinking EDM machine Servspark Eletroplus 540 model. Some modifications were carried out on the machine to enable the application of the boriding process by EDM; similar to what was proposed by other researchers^{32,33} when the nitriding method by die-sinking EDM was applied.

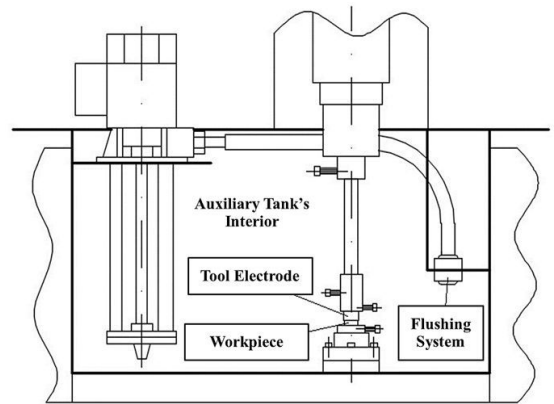


Figure 4. EDM machine's auxiliary tank (Authors, 2022).

2.1. EDM machine modifications and preparation for the boriding process

A 304 austenitic stainless steel auxiliary tank was manufactured and installed inside the EDM machine main work tank (Figure 4). The Figure 4 also highlights the schematic drawing of the tank interior with the tool and workpiece assembled to the electrode holder and sample holder, respectively, as well as it shows the flushing system. The auxiliary tank prevents contamination of the dielectric fluid of the machine with aqueous dielectric fluids used during the EDM process. A centrifugal pump was assembled in the auxiliary tank to enable the flushing and cleaning of the work gap using the same dielectric fluid solution, which is deionized water with sodium octaborate ($Na_2B_8O_{13} \cdot 4H_2O$).

AISI 4140 steel samples (19.00 mm diameter and 13.00 mm thickness) were used as base material and workpiece, since this material is extensively used in automotive components in the boriding condition³⁴. As tool electrodes, it was employed cylindrical electrolytic copper samples (22.00 mm diameter and 30.00 mm length). Table 1 presents the AISI 4140 steel chemical composition (wt. %), performed using an optical emission spectrometer (OES) SPECTROMAXx, model LMXM5M-BT.

The dielectric fluid was prepared with 30 liters of water obtained from public supply, which had high initial electrical conductivity ($160 \mu S cm^{-1}$) and was therefore deionized using a resin-based portable deionizer, reaching the value

Table 1. Chemical composition (wt. %) of AISI 4140 steel used as base material.

Element	C	Mn	P	S	Si	Cr	Mo	Fe
Wt. %	0.402	0.803	0.012	0.003	0.327	0.893	0.183	Balance

of $0 \mu\text{S cm}^{-1}$. Sodium octaborate ($\text{Na}_2\text{B}_8\text{O}_{13} \cdot 4\text{H}_2\text{O}$) was diluted in deionized water to form an aqueous solution at a concentration of 16.6 g L^{-1} .

Table 2 shows the operating parameters adjusted in the die-sinking EDM machine that enabled the application of the EDM boriding process. The test duration for each sample was 10 minutes.

2.2. Techniques and mechanical tests used in the work after the EDM process

The recast and intermediate layers hardness, as well as the substrate hardness, were measured by the Vickers method in a Shimadzu HMV-2T E microhardness tester with a load of $25 \text{ gf}^{0.35}$ and dwell time of 15 seconds. The hardness indentations were performed in the sample's cross-sections following a minimum indent spacing of $20 \mu\text{m}$ and were repeated three times. Hardness profiles were performed with the aid of images obtained by optical microscope with Easy Test HMV-AD software incorporated into the microhardness tester in order to verify the behavior of the hardness when moving away from the surface. Micrographs of the recast layers and intermediate layers were obtained using an optical microscope incorporated at the microhardness tester.

X-ray diffraction with Bragg-Brentano (θ - 2θ) configuration was used to identify the presence of iron borides. Table 3 shows the diffractometer technical specifications used in the work. Before performing the XRD analyses, the samples were previously cleaned with alcohol in an ultrasound device for 15 min.

Scanning Electron Microscopy (SEM) was employed to obtain images of the samples cross-section using the Shimadzu SSSX-150 model to evaluate the altered layers after the EDM process. The Energy Dispersive X-ray Spectroscopy (EDS) analyses were performed in regions of the recast and intermediate layers to investigate the presence of the boron element.

3. Results and Discussion

Figure 5 shows the proposed model to represent the boriding phenomena through die-sinking electrical discharge machining. At the beginning of the process (ignition phase of the plasma channel), the potential difference or voltage (Volts) generated in the electric field accelerates the electrons from the cathode, which on their way towards the anode, collide with the molecules present in the dielectric fluid. Such collisions are energetic enough to ionize the compounds present in the aqueous medium. Consequently, from the moment that the plasma channel is established, the B^{3+} ions (originated from the impact ionization process) are accelerated towards the cathode (AISI 4140 steel), thus resulting in the workpiece surface boriding by EDM.

According to Yerokhin et al.³⁶, in the electrolytic plasma process, nitrogen and carbon atoms are transferred from the electrolyte to the surface. The diffusion of the elements that

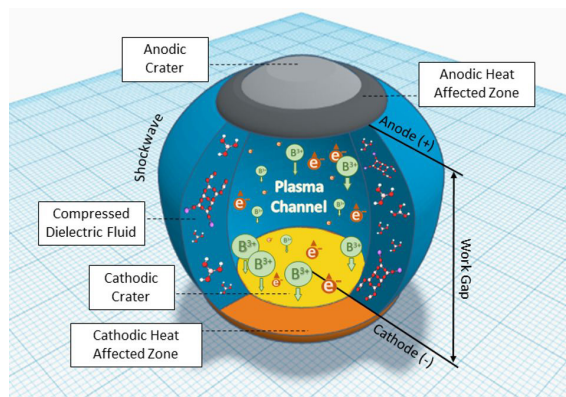
Table 2. Operational parameters used for the EDM process.

Parameter	Specification
Dielectric fluid	Sodium octaborate ($\text{Na}_2\text{B}_8\text{O}_{13} \cdot 4\text{H}_2\text{O}$)
Dielectric concentration	$16.6 \text{ [g L}^{-1}\text{]}$
Tool	Electrolytic copper
Tool polarity	Positive [+]
Peak current	40 [A]
Pulse-on time (T_{ON})	$500 \text{ [}\mu\text{s]}$
Pulse-off time (T_{OFF})	1.5^*
Gap	1.0^*
Periodic tool retraction	5.0^*
Servo speed	5.0^*
Erosion time	5.0^*
Test duration per each sample	10.0 [mm]

* Fixed values adjusted on the EDM machine panel.

Table 3. Selected parameters for XRD analyses.

Parameter	Specification
X-ray source	Cu $\text{K}\alpha 1$ radiation ($\lambda = 1.5406 \text{ \AA}$)
X-ray tube voltage	40 kV
X-ray tube current	30 mA
Method	Bragg Brentano (θ - 2θ)
Range (2θ)	20° to 120°
Scan mode	Fixed time
Scan step size	0.04°
Collection time	1 s

**Figure 5.** Schematics of the proposed model for the boriding process by EDM. (Authors, 2022).

compose the electrolytic fluid is possible due to the plasma channel created along the electrode surface, allowing the formation of metastable phases in the microstructure due to thermochemical reactions. The hypothesis of implantation of boron in the material is pertinent since there is a source of boron in the aqueous solution formed by sodium octaborate diluted in deionized water. The plasma channel energy is sufficient to decompose the constituents present in the boric acid solution and release the positive boron ions according to the reactions presented in the introduction of this article. During the discharge period, the energy irradiating from the plasma channel causes ionization, dissociation, and vaporization of the molecules in the electrolytic fluid surrounding the channel. When discharge time ends, due to the decrease in energy flow reaching the electrodes, the molten craters begin to solidify. The model represented in the figure is similar to the boron transfer mechanism presented in the conventional plasma boriding process. The positive ions accelerated towards the surface of the cathode, promoting heating and discontinuity in the network due to the bombardment of the ions, which are implanted in the microstructure of the treated material.

Özerkan³⁷ conducted a study on the EDM machining process using boron powder, and obtained good results with

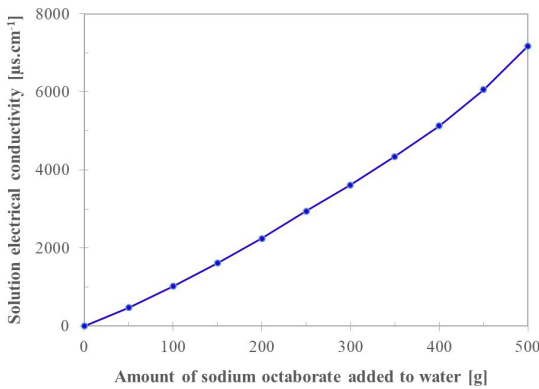


Figure 6. Variation of solution electrical conductivity as a function of the amount of sodium octaborate added to deionized water.

the boron implantation on the machined by EDM material surface. The EDM boriding process takes place in short times (μs), simultaneously reconciling boriding with the machining of the workpiece. The process is simple, easy to manage and requires little maintenance, depending on just a few adaptations in the EDM machine. The EDM boriding process had to act in a dielectric fluid with high conductivity, composed of deionized water and sodium octaborate. Despite using deionized water ($0 \mu\text{S cm}^{-1}$), when sodium octaborate (source of boron) was added in the fluid, the conductivity of the solution grows exponentially (Figure 6), reaching a value of $7000 \mu\text{S cm}^{-1}$, approximately. Santos et al.³⁸, faced a similar challenge, as when they mixed up to 12.5 g l^{-1} urea in deionized water, they found electrical conductivity of 4 to $1570 \mu\text{S cm}^{-1}$.

Figure 7 shows the AISI 4140 steel cross-section borided by EDM with dielectric fluid composed of sodium octaborate ($\text{Na}_2\text{B}_8\text{O}_{13}\cdot 4\text{H}_2\text{O}$) added to deionized water and using electrolytic copper as a tool electrode. Figure 7(a) shows the formation of the recast and borided (intermediate) layers, similar to what³⁸ observed in the nitriding by EDM process. Part of the recast layer fractured and detached from the sample surface, and its layer was not uniform. Instead, the intermediate layer appeared in the entire sample cross-section. Figure 7(b) shows the SEM image of the AISI 4140 steel sample cross-section borided by EDM. The authors also noted the difference between the indentation sizes produced by Vickers microhardness, with emphasis on the two indentations in the base material, whose sizes are larger than the ones on the modified layer. This occurs due to the increase in hardness provided by the boriding process, as also reported by³⁹.

Table 4 shows the Vickers microhardness (25 gf, 15 s) of the AISI 4140 steel layer borided by EDM with an electrolytic copper tool. Note that there are gains of 146.8% and 185.8% in the hardness of the borided (intermediate) and recast layers, respectively. The increase in hardness of the recast layer is due to metallurgical changes provided by heating followed by suddenly cooling that comes from dielectric fluid, as reported by⁴⁰.

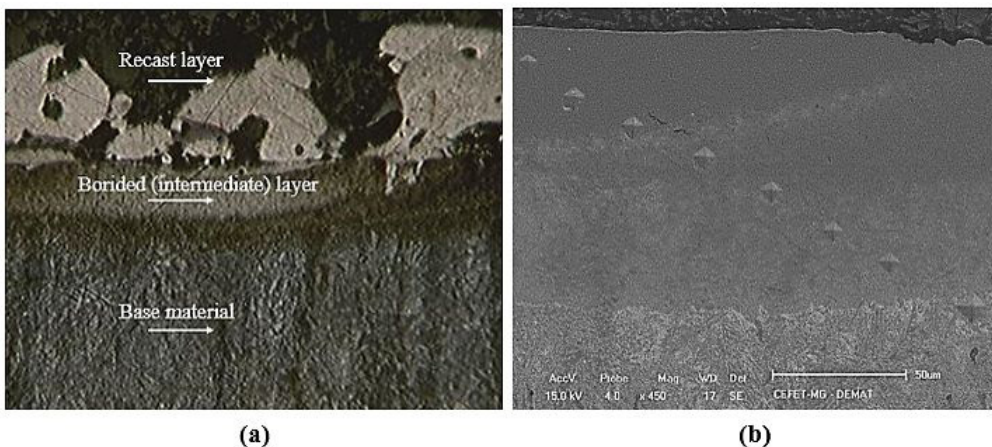
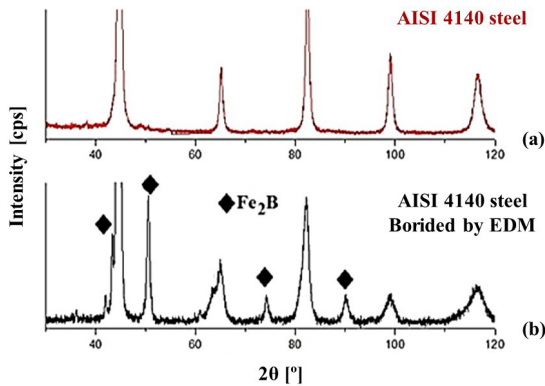


Figure 7. Cross-section of AISI 4140 steel borided by EDM with electrolytic copper tool electrode: (a) optical microscopy image (Nital 3%); (b) SEM image.

Table 4. Vickers microhardness of AISI 4140 steel (base material), and of borided and recast layers.

	AISI 4140 steel (base material)	Borided (intermediate) layer	Recast layer
Microhardness (HV)	288.8 ± 18.2	712.8 ± 83.1	825.4 ± 73.4
Increase in hardness	-	146.8%	185.8%

**Figure 8.** X-ray diffractograms of the AISI 4140 steel (base material) and of the borided by EDM sample with a copper tool

In order to investigate the reason for the hardness increase on the AISI 4140 steel borided by EDM, it was performed X-ray diffraction on the samples cross-sections, as shown in Figure 8. Note that the iron boride peaks are shown in the EDM processed sample when compared to AISI 4140 steel (base material), which is similar to that reported by³. The most intense peaks of the diffractogram are similar to the ones observed by⁴¹, which found the Fe_2B iron borides, as well as similar results were found by⁴². This occurs due to the collision mechanism of ions and electrons that caused the rupture of the dielectric fluid, with enough energy to decompose the constituents present in the solution (sodium octaborate mixed in deionized water) and enable the addition of boron to the surface through the plasma channel. The insertion of boron, which resulted in iron borides, can explain the increase in surface hardness³, as reported by⁴, an increase of up to 5 times the surface hardness as a result of the boriding process at 1000 °C for 4 h. The increase in hardness values shown in Table 3 can be attributed to the borided layer produced, as also noted by⁴³. A borided layer thickness of approximately 50.6 μm can also be seen in Figure 4, corroborating the data from³⁵, which obtained a borided layer of approximately 51 μm on PM HSS AISI M2 steel. While⁴⁴ obtained experimentally a Fe_2B boriding layer thickness from 20 to 160 μm when both the process temperature and treatment time varied from 850 to 1000 °C and from 2 to 8 hours, respectively. Zuno-Silva et al.⁴⁵, obtained equivalent results and noted a Fe_2B layer thickness increase with treatment time, and obtained a layer thickness from $41.93 \pm 8.25 \mu\text{m}$ for 2 h to $95.48 \pm 17.4 \mu\text{m}$ for 8 h at 900 °C.

Corroborating the data from^{41,46}, the results indicated that the boriding process is possible by employing adapted EDM equipment, similar to what was observed by³² when they used the EDM machine to nitride AISI 4140 steel, and by³⁰ when they investigated the formation of the nitride

layer in AISI H13 steel machined by die-sinking EDM. The borides produced by the chemical reaction between the AISI 4140 steel and the boron element, decomposed from sodium octaborate ($\text{Na}_2\text{B}_8\text{O}_{13} \cdot 4\text{H}_2\text{O}$) in deionized water, indicated the feasibility of surface modification of the AISI 4140 steel through the EDM adapted machine.

4. Conclusions

Based on the results obtained in this work, it can be drawn the following conclusions:

- The methodology applied in this work by using adapted die-sinking Electrical Discharge Machining (EDM) equipment, with sodium octaborate ($\text{Na}_2\text{B}_8\text{O}_{13} \cdot 4\text{H}_2\text{O}$) as dielectric fluid, allowed obtaining higher hardness in the AISI 4140 steel surface and subsurface compared to the base material.
- It was able to obtain microhardness gains of 146.8% and 185.8% for the intermediate and recast layers, respectively, compared to AISI 4140 steel (base material), which suggests the presence of iron borides (Fe_2B) identified by X-ray diffraction.
- The presence of this phase can be explained by the chemical element boron (decomposed from sodium octaborate, $\text{Na}_2\text{B}_8\text{O}_{13} \cdot 4\text{H}_2\text{O}$, mixed with deionized water), which was observed in the produced layers through the obtained SEM-EDS spectrum.
- It was able to use optical microscopy images to observe the uniformity of the borided (intermediate) layer, which differed from the recast layer that detached from the AISI 4140 steel sample surface.
- The high electrical conductivity value obtained for the sodium octaborate diluted in deionized water (approximately 7000 $\mu\text{S}/\text{cm}$) resulted in difficulty in carrying out the process. However, it did not prevent the boriding by EDM in AISI 4140 steel.

5. Acknowledgments

The authors thank the Postgraduate Program in Materials Engineering (POSMAT) of the Federal Center for Technological Education of Minas Gerais (CEFET-MG), Brazil, for the provision of laboratory facilities.

6. References

1. Türkmen İ, Yalamaç E. Effect of alternative boronizing mixtures on boride layer and tribological behavior of boronized SAE 1020 steel. *Met Mater Int.* 2022;28(5):1114-28.
2. Chen T, Foo C, Tsang SCE. Interstitial and substitutional light elements in transition metals for heterogeneous catalysis. *Chem Sci.* 2021;12(2):517-32.
3. Gunes I, Taktak I, Bindal C, Yalcin Y, Ulker S, Kayali Y. Investigation of diffusion kinetics of plasma paste borided AISI 8620 steel using a mixture of B_2O_3 paste and $\text{B}_4\text{C}/\text{SiC}$. *Sadhana Acad Proc Eng Sci.* 2013;38(3):513-26.

4. Sen S, Sen U, Bindal C. An approach to the kinetic study of borided steels. *Surf Coat Tech.* 2005;191(2-3):274-85.
5. Kulka M. Current trends in boriding. Cham: Springer International Publishing; 2019.
6. Sinha AK. Boriding (boronizing). In: ASM International, editor. ASM handbook. Materials Park; 1991. p. 437-47. (vol. 4).
7. Pfender E, Boulos M, Fauchais P, Feinman J. Methods and principles of plasma generation. In: Feinman J, editor. Plasma technology in metallurgical processing. Warrendale: Iron and Steel Society; 1987. p. 27-47.
8. Fauchais P, Boulos M, Pfender E. Physical and thermodynamic properties of thermal plasmas. In: Feinman J, editor. Plasma technology in metallurgical processing. Warrendale: Iron and Steel Society; 1987. p. 11-26.
9. Frank-Kamenetskii D. Plasma: the fourth state of matter. New York: Springer Science & Business Media; 2012.
10. Santos CA. Composição superficial e propriedades mecânicas e tribológicas de aços carbono implantados com nitrogênio [thesis]. Porto Alegre: Curso de Pós-graduação em Física, Instituto de Física, Universidade Federal do Rio Grande do Sul; 1984.
11. Chapman B, Vossen JL. Glow discharge processes: sputtering and plasma etching. *Phys Today.* 1981;34(7):62.
12. Basso RLO. Efeito do carbono no processo de nitrocarburização com plasma pulsado da liga metálica AISI H13. [thesis]. Campinas: Instituto de Física Gleb Wataghin, Universidade Estadual de Campinas; 2007.
13. Mehrer H. Diffusion in solids: fundamentals, methods, materials, diffusion-controlled processes. Berlin: Springer Science & Business Media; 2007.
14. Kaestner P, Olfe J, Rie KT. Plasma-assisted boriding of pure titanium and TiAl6V4. *Surf Coat Tech.* 2001;142:248-52.
15. Dearnley PA, Farrell T, Bell T. Developments in plasma boronizing. *J Mater Energy Syst.* 1986;8(2):128-31.
16. Porter DA, Easterling KE. Phase transformations in metals and alloys. Boca Raton: CRC Press; 2009.
17. Keddad M, Taktak S. Characterization and diffusion model for the titanium boride layers formed on the Ti₆Al₄V alloy by plasma paste boriding. *Appl Surf Sci.* 2017;399:229-36.
18. Martini C, Palombarini G, Carbuicchio M. Mechanism of thermochemical growth of iron borides on iron. *J Mater Sci.* 2004;39(3):933-7.
19. Fridman A. Plasma chemistry. Cambridge: Cambridge University Press; 2008.
20. Gupta P, Tenhundfeld G, Daigle EO, Ryabkov D. Electrolytic plasma technology: science and engineering: an overview. *Surf Coat Tech.* 2007;201(21):8746-60.
21. Taktak S. Some mechanical properties of borided AISI H13 and 304 steels. *Mater Des.* 2007;28(6):1836-43.
22. Gupta P, Tenhundfeld G, Daigle EO, Ryabkov D. Electrolytic plasma technology: science and engineering - An overview. *Surf Coat Tech.* 2007;201(21):8746-60.
23. Akyüz O, Tek Z. Mechanical properties of boronized 2365 steel by pulsed plasma-electrolysis technique. *Mater Sci Eng B.* 2015;5(1-2):50-7.
24. Sireli GK. Molten salt baths: electrochemical boriding. In: Colás R, Totten GE, editors. Encyclopedia of iron, steel, and their alloys. Boca Raton: Taylor & Francis; 2016. p. 2284-300.
25. Jiang Y, Bao Y, Wang M. Kinetic analysis of additives on plasma electrolytic boriding. *Coatings.* 2017;7(5):61.
26. Ekmekci B. Residual stresses and white layer in electric discharge machining (EDM). *Appl Surf Sci.* 2007;253(23):9234-40.
27. König W. Fertigungsverfahren 3: abtragen und generieren. Berlin: Springer-Verlag; 2013.
28. Kumar S, Singh R, Singh TP, Sethi BL. Surface modification by electrical discharge machining: a review. *J Mater Process Technol.* 2009;209(8):3675-87.
29. Ekmekci B, Elkoca O, Erden A. A comparative study on the surface integrity of plastic mold steel due to electric discharge machining. *Metall Mater Trans, B, Process Metall Mater Proc Sci.* 2005;36(1):117-24.
30. da Silva SP, Abrão AM, Weidler PG, Silva ER, Câmara MA. Investigation of nitride layers deposited on annealed AISI H13 steel by die-sinking electrical discharge machining. *Int J Adv Manuf Technol.* 2020;109(7-8):2325-36.
31. Yan BH, Tsai HC, Huang FY. The effect in EDM of a dielectric of a urea solution in water on modifying the surface of titanium. *Int J Mach Tools Manuf.* 2005;45(2):194-200.
32. Santos RF, Silva ER, Sales WF, Raslan AA. Influence of the electrode material on the nitriding of medium carbon steel using sink electrical discharge machining. *Int J Adv Manuf Technol.* 2017;90(5-8):2001-7.
33. Silva SP, Abrão AM, Silva ER, Câmara MA. Surface modification of AISI H13 steel by die-sinking electrical discharge machining and TiAlN coating: a promising hybrid technique to improve wear resistance. *Wear.* 2020;462-463:203509.
34. Ulutan M, Yildirim MM, Çelik ON, Buytoz S. Tribological properties of borided AISI 4140 steel with the powder pack-boriding method. *Tribol Lett.* 2010;38(3):231-9.
35. Arcego ML, Milan JCG, da Costa CE, de Almeida EA S. Effect of boride layer on PM HSS AISI M2 on the mechanisms acting in the transverse. *Mater Res.* 2018;21(1):e20170160.
36. Yerokhin AL, Nie X, Leyland A, Matthews A, Doney SJ. Plasma electrolysis for surface engineering. *Surf Coat Tech.* 1999;122(2-3):73-93.
37. Özerkan HB. Simultaneous machining and surface alloying of AISI 1040 steel by electrical discharge machining with boron oxide powders. *J Mech Sci Technol.* 2018;32(9):4357-64.
38. Santos RF, da Silva ER, Sales WF, Raslan AA. Influence of urea content blended with deionized water in the process of nitriding using electrical discharge machining on AISI 4140 steel. *Int J Adv Manuf Technol.* 2016;89(1-4):1251-7.
39. Lou DC, Solberg JK, Akselsen OM, Dahl N. Microstructure and property investigation of paste boronized pure nickel and Nimonic 90 superalloy. *Mater Chem Phys.* 2009;115(1):239-44.
40. Ghanem F, Braham C, Fitzpatrick ME, Sidhom H. Effect of near-surface residual stress and microstructure modification from machining on the fatigue endurance of a tool steel. *J Mater Eng Perform.* 2002;11(6):631-9.
41. Yao Q, Sun J, Fu Y, Tong W, Zhang H. An evaluation of a borided layer formed on Ti-6Al-4V alloy by means of SMAT and low-temperature boriding. *Materials.* 2016;9(12):993.
42. An J, Li C, Wen Z, Yang YL, Sun SJ. A study of boronizing of steel AISI 8620 for sucker rods. *Metal Sci Heat Treat.* 2012;53(11-12):598-602.
43. Ulutan M, Celik ON, Gasan H, Er U. Effect of different surface treatment methods on the friction and wear behavior of AISI 4140 steel. *J Mater Sci Technol.* 2010;26(3):251-7.
44. Mebarek B, Benguelloula A, Zanoun A. Effect of boride incubation time during the formation of Fe₂B phase. *Mater Res.* 2018;21(1):1-7.
45. Zuno-Silva J, Keddad M, Ortiz-Dominguez M, Elias-Espinosa MC, Cervantes-Sodi F, Oseguera-Peña J, et al. Kinetics of formation of Fe₂B layers on AISI S1 steel. *Mater Res.* 2018;21(5):1-10.
46. Joshi AA, Hosmani SS. Pack-boronizing of AISI 4140 steel: boronizing mechanism and the role of container design. *Mater Manuf Process.* 2014;29(9):1062-72.1.